

## Recent Results from the Goldstone Orbital Debris Radar: 2016-2017

James Murray<sup>(1)</sup>, Rossina Miller<sup>(1)</sup>, Mark Matney<sup>(2)</sup>, Phillip Anz-Meador<sup>(1)</sup>, Timothy Kennedy<sup>(2)</sup>

<sup>(1)</sup>Jacobs, NASA Johnson Space Center, Mail Code XI5-9E, 2101 NASA Parkway, Houston, TX 77058, USA,  
james.i.murray@nasa.gov

<sup>(2)</sup>NASA Johnson Space Center, Mail Code XI5-9E, 2101 NASA Parkway, Houston, TX 77058, USA

### ABSTRACT

Since 1993, the NASA Orbital Debris Program Office has used the Goldstone Orbital Debris Radar (Goldstone) to sample statistically the orbital debris environment. Due to the sensitivity of this radar, which can detect an approximately 3 mm-diameter conducting sphere at 1,000 km, it has filled an important role in the characterization of the sub-centimeter-sized orbital debris population. Through the years, the capabilities of this system have increased – recent updates include increased receiver bandwidth and a change in the bi-static observation geometry – both of which enhance the radar’s ability to estimate orbital parameters. In 2016, dual polarization capability was added, making this the first year where both right- and left-hand circularly polarized information was available from this sensor. This additional polarization information may enable better characterization of sub-centimeter-sized particles in low Earth orbit, particularly since the receiver triggers on reflected energy from both left- and right-handed circular polarizations independently.

In this paper, we present measurements and results derived from data taken during the calendar years (CY) 2016-2017 by Goldstone and compare this dataset to measurements taken by the Haystack Ultra-wideband Satellite Imaging Radar (HUSIR) during a similar timeframe.

### 1 INTRODUCTION

The NASA Orbital Debris Program Office (ODPO) makes measurements of the current orbital debris environment one of its main objectives. These data are used to build, verify, and validate models of the current and future debris environment. Measurements have also proven valuable in identifying previously unknown sources of orbital debris.

The NASA ODPO uses a variety of instruments to measure the orbital debris environment. In low Earth orbit (LEO), objects with diameters larger than 10 cm to 30 cm are tracked by the by U.S. Space Surveillance Network (SSN). For objects smaller than ~3 mm in diameter, *in-situ* data are available from analysis of returned surfaces from space, such as the Hubble Space Telescope’s Wide Field and Planetary Camera 2 [1]. Since 1990, NASA has used the Haystack Ultra-wideband Satellite Imaging Radar (HUSIR) to measure the LEO environment. Formerly known as the Haystack Long Range Imaging Radar, HUSIR is operated by the Massachusetts Institute of Technology Lincoln Laboratory. HUSIR can measure debris objects with a diameter as small as approximately 5 mm at an altitude of 1000 km.

This still leaves a gap in our knowledge of objects in the 1 mm to 5 mm diameter range. Although these particles are small, this size regime is where many spacecraft are susceptible to significant damage from collisions [2]. It is in this size regime that the Goldstone Orbital Debris Radar (Goldstone) contributes to our understanding of the orbital debris environment.

Since 1993, Goldstone has collected orbital debris data in LEO for debris as small as approximately 2 mm, depending on altitude, for the NASA ODPO. Goldstone is an extremely sensitive sensor capable of detecting a 3 mm metallic sphere at 1000 km [3], which makes it an incredibly useful tool in the characterization of the sub-centimeter-sized debris population in LEO. This paper summarizes the results of Goldstone observations made during CY16–17.

### 2 GOLDSTONE RADAR SYSTEM OVERVIEW

Goldstone is located in the Mojave Desert near Barstow, California (35° 25' 33" N and 243° 6' 38" 53' 24" W) at an altitude of 900 m above mean sea level. The radar is part of the larger Goldstone Deep Space Communications Complex (GDSCC) operated by the NASA Jet Propulsion Laboratory (JPL). The GDSCC is one of three sites in the

NASA Deep Space Network. The main purpose of these sites is to communicate with and track space missions, many of them in deep space; therefore, they are equipped with large, powerful, transmitters and very sensitive receivers to carry out their mission.

Until recently, NASA ODPO has made use of antennas DSS-14 (“Mars”) and DSS-15 (“Uranus”) when they are available, for orbital debris bi-static data collection. DSS-14 is a 70-meter Cassegrain reflector antenna used to transmit a frequency modulated “chirp” waveform. Approximately 500 meters away, DSS-15, a 34-meter “High Efficiency” reflector, listens for the return signals reflected off orbital debris traversing the beam.

The radar is operated in a fixed, staring mode and does not attempt to track objects in the beam. In the past, Goldstone has aimed DSS-14 at 1.5 degrees from the zenith towards the back of DSS-15 at 154.6 degrees azimuth. DSS-15 was aimed at 1.441 degrees from the zenith and at the same azimuth as the transmitter in order to overlap their beams. In this configuration the half-power (3 dB) beamwidth of the two antennas intersect from 280 km to about 3000 km altitude, as shown in Fig.1.

Because of this geometry, the cross-section of the beam is a function of both the range of the target and the path of the debris motion through the beam. In addition, larger objects may be detected if they miss the main beam but pass through one of the antenna sidelobes. Such sidelobe detections usually can be identified because their signal persists over a longer time interval than the nominal duration of a main-beam crossing, about 90 milliseconds. There is no monopulse capability on the radar to determine how close the object passes to the center of the beam.

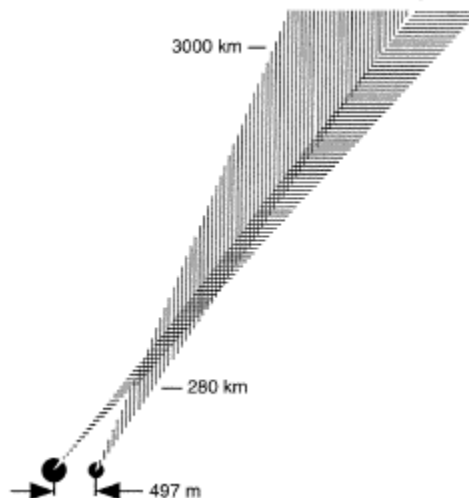


Fig.1. Illustrative example of transmitting and receiving antennas’ beams. The crosshatched section indicates the region of overlap between the two beams. [4]

Goldstone is an X-band radar transmitting at a center frequency of 8560 MHz corresponding to a wavelength of 3.502 cm. The waveform utilized by Goldstone for orbital debris observations is a linear frequency modulated (LFM) waveform or chirp. Following an upgrade to a wideband system in June 2011, the chirp bandwidth increased from 46.15 kHz to 300 kHz. The radar alternates between transmitting an up-chirp and a down-chirp with a receive window in between. For a detection to be declared, the received signal power must exceed the specified threshold on both the up- and down-chirp. After transmission of the up-chirp, the receiver is turned off for approximately 0.15 milliseconds to prevent saturation of the receiver caused by returns from nearby structures, then turned on for 20 milliseconds to listen for echoes off debris objects in the beam. Then, this cycle is repeated with the radar transmitting a down-chirp instead of an up-chirp. The whole cycle takes approximately 45 milliseconds. This strategy permits the separate measurement of range and range-rate, if only one object is in the beam at a time.

The signal-to-noise ratio threshold is chosen such that a random noise spike would produce a false detection on an average of once per 28 hours. Once a threshold crossing is identified in succeeding transmitted chirps (the detection can begin on either an up- or a down-chirp), the range is estimated by averaging the apparent ranges of the two

responses. Similarly, the Doppler is calculated by taking the difference between the measured Doppler responses on the up- and down-chirps. Using two succeeding pulses with opposite frequency slopes allows the signal processor to negate the effects of range-Doppler coupling on an LFM chirp and to determine the true range and Doppler frequency.

## 2.1 Operating Parameter Changes

Starting on 27 December 2007, Goldstone began pointing in a new staring geometry aiming the transmitter, DSS-14, at 75° elevation from the horizon and 90° azimuth (due east) with respect to local north. The receiver, DSS-15, was aimed a fraction of a degree above 75° elevation and less than half of a degree north of due east (effectively 89.8° azimuth at 550 km slant range). This allows for a range extent from 374 km to 3373 km and for a measurement of the radial velocity or range-rate of the detection that allows for a better orbital inclination calculation (assuming a circular orbit). This observation configuration is referred to as 75E and mimics the main observation geometry used by HUSIR for debris observations. Table 1 summarizes the changes to the operational parameters associated with the system bandwidth upgrade.

Table 1. Transmit Waveform Details Pre- and Post-upgrade to a Wideband System in June 2011

	PRE-WIDEBAND UPGRADE	POST-WIDEBAND UPGRADE
<b>BANDWIDTH (KHZ)</b>	46.15	300
<b>SAMPLING PERIOD (μSEC)</b>	19.5	.66
<b>PULSE DURATION (SAMPLES)</b>	120	3510

Nominal orbital debris operations involve transmitting a right circularly polarized (RCP) waveform and receiving a left circularly polarized (LCP) waveform, referred to as the principal polarization (PP). Until December 2015, Goldstone recorded only the PP detection channel (LCP); however, beginning with the data collection window on 15 December 2015, Goldstone has delivered both PP (LCP) and orthogonal polarization OP (RCP) detection data.

## 3 MEASUREMENTS

Orbital debris data is collected at Goldstone on an as available basis. The data is processed by NASA JPL personnel and reviewed by a subject matter expert before being delivered to the NASA ODPO at Johnson Space Center. The table below summarizes the total hours collected at 75E for the period covered in this report.

Table 2. Summary of Measurements taken by Goldstone in CY16–17

CALENDAR YEAR	TOTAL HOURS OBSERVED (HRS)	TOTAL NUMBER OF DETECTIONS (#)	AVERAGE COUNT RATE (#/HR)
2016	46.3	3427	74.0
2017	51.8	3064	59.1

The average count rate in 2017 is lower than that in 2016. This is because for 2016 and the first half of 2017, Goldstone was operating at nominal transmission power, 440 kW. For the latter half of 2017, Goldstone operated at a much lower transmission power, approximately 240 kW, reducing its ability to detect smaller debris objects, particularly at higher altitudes.

Figure 2 shows the orbit altitude versus Doppler inclination for debris detected by Goldstone in CY16-17. The Doppler inclination is calculated using the radar geometry and measured range and range-rate, assuming a circular orbit. The same debris clouds identified in HUSIR data are present [5]. The most prominent are those between 94° and 105° associated with the sun-synchronous family of orbits; 71° and 78°, associated with the Cosmos 2251 cloud from its collision with Iridium 33; 63° and 67°, associated with the sodium-potassium (NaK) coolant droplets ejected from Radar Ocean Reconnaissance Satellite (RORSAT) nuclear reactors; and the family of debris in the 81° to 87° inclination band, which was identified in recent HUSIR data.

Additionally, a family of debris not visible in normal HUSIR debris data collects is present above 2500 km in altitude and seen across a wide band of Doppler inclinations. It has been suggested by [6] that the population may be remnants of Project Westford, in which two Atlas Agena launch vehicles – one on 21 October 1961 and one on

9 May 1963 – carried special canisters of densely packaged, very thin wires to act as dipole reflectors of X-band transmissions. The orbit and design of the individual needles were chosen to promote rapid orbital decay and reentry into the atmosphere. These needles are believed to have reentered within a few years of launch, largely due to solar radiation pressure effects. However, due to design characteristics and unanticipated thermal effects, the needles did not all dispense individually as planned but instead in clumps of needles. There are currently 46 clumps of needles cataloged by the SSN. The population identified in Fig. 2 may represent clumps too small to be tracked by the SSN or needles released from existing clumps. The wide band in Doppler inclinations is a manifestation of the non-zero eccentricity of this population. The addition of the complete PP/OP signals from Goldstone offers a new tool to study this Westford needle population.

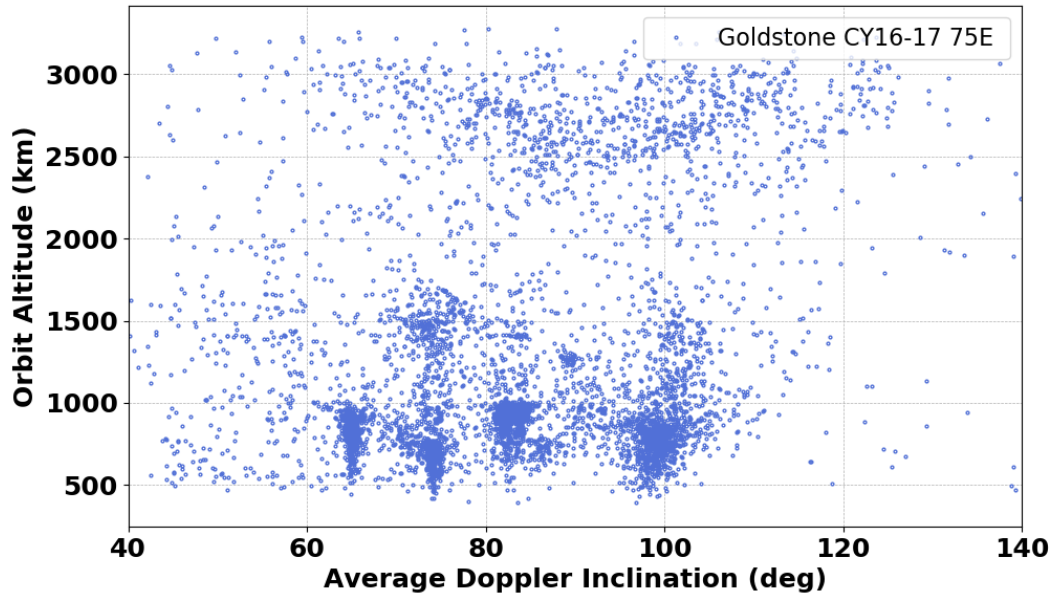


Fig. 2. Orbit altitude versus average Doppler inclination for debris detected by Goldstone in CY16-17. The Doppler inclination is calculated using the radar geometry and measured range and range-rate, assuming a circular orbit.

### 3.1 The NASA Size Estimation Model

The NASA Size Estimation Model (SEM) was developed to relate radar cross-section (RCS) to the physical size of an on-orbit debris fragment [7]. The characteristic length of an object is defined as the average of the largest dimensions for an object measured along three orthogonal axes. The first axis was chosen to coincide with the largest dimension, the second axis to coincide with the largest dimension in a plane orthogonal to the first axis, and the third axis to be orthogonal to the plane defined by the first two axes. The characteristic length of an object is referred to interchangeably as size or diameter.

In Fig. 3 the results of RCS-to-size measurements on 39 representative debris objects are shown, where each point represents an average RCS over many orientations for a single object measured at a single frequency. The oscillating curve is the RCS for a spherical conductor while the smooth curve is the fit to the data and comprises the NASA SEM.

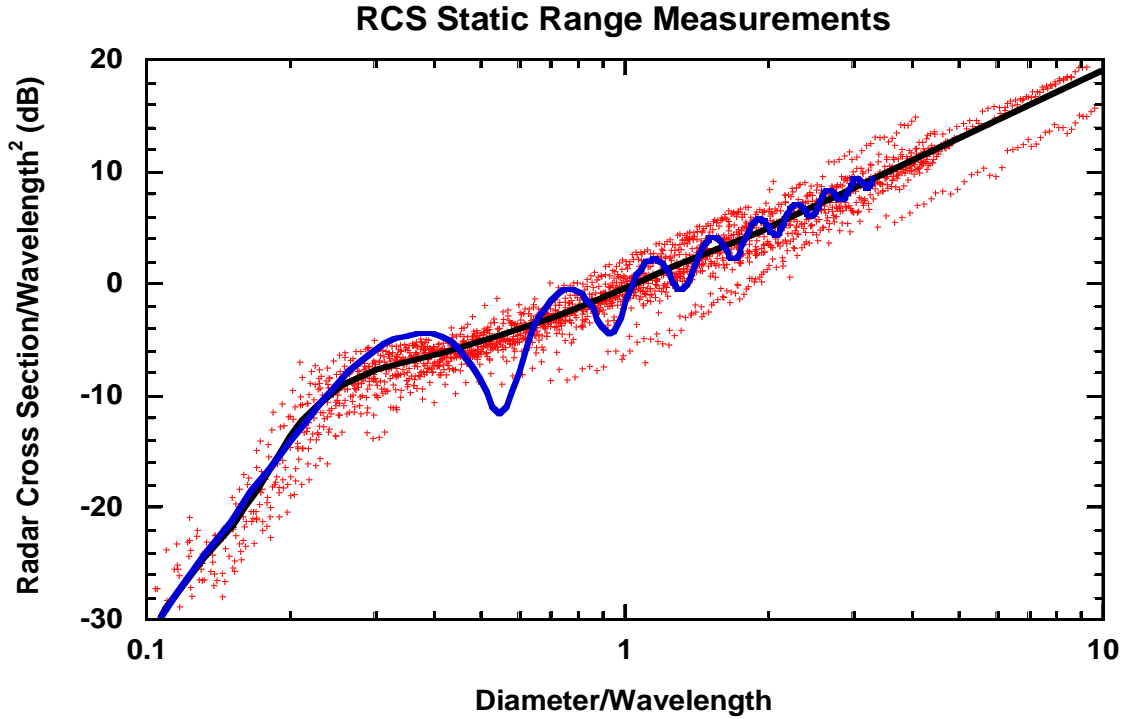


Fig. 3. Results of RCS-to-size measurements on 39 representative debris objects. The oscillating line is the RCS for a spherical conductor while the smooth line is the fit to the data.

#### 4 DATA CALIBRATION USING NaK COOLANT DROPLETS

In previous studies [8-10], highly PP-polarized debris ( $P \approx 1$ ) with inclinations near  $65^\circ$  and an altitude between 700 km and 1000 km were identified as spherical, eutectic NaK nuclear reactor coolant droplets from the ejected core of RORSATs, where the polarization ( $P$ ) is defined as:

$$P = \frac{RCS_{PP} - RCS_{OP}}{RCS_{PP} + RCS_{OP}} \quad (\text{Eq. 1})$$

In contrast to debris in other altitude and inclination bands, which exhibit a wide polarization distribution, the NaK population, being composed of small metallic spheres, exhibits highly polarized signatures. Orbital debris observations in polarization and RCS space, after filtering on altitude less than 1000 km and Doppler inclination between  $62.9^\circ$  and  $67^\circ$  for radar observations from CY16–17 are shown in Fig. 4 and 5. The dashed black lines represent an ad-hoc polarization threshold developed to separate the highly polarized cluster of NaK from the rest of the orbital debris population in this altitude and Doppler inclination region. Such decision boundaries are sensor dependent, and a separate polarization threshold was developed for HUSIR [5].

For this and all subsequent plots, Goldstone CY17 data is split into CY17 A, where Goldstone was operated at nominal transmission power, and CY17 B, where Goldstone was operated with significantly reduced transmission power.

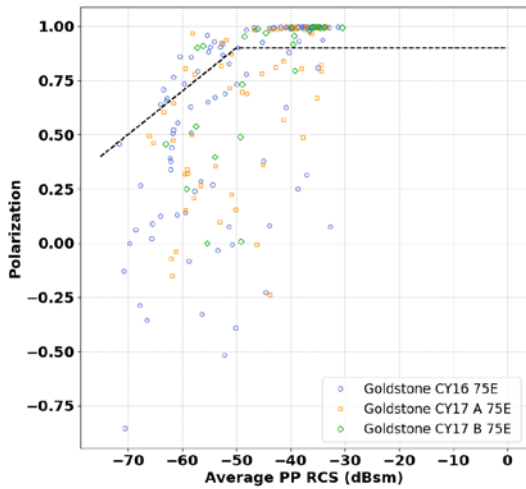


Fig. 4. Polarization versus average PP RCS for debris objects detected by Goldstone with altitude < 1000 km and  $62.9^\circ < \text{Doppler inclination} < 67^\circ$  in CY16–17.

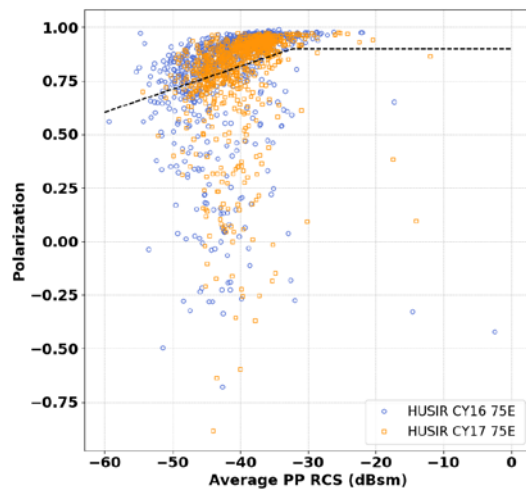


Fig. 5. Polarization versus average PP RCS for debris objects detected by HUSIR with altitude < 1000 km and  $62.9^\circ < \text{Doppler inclination} < 67^\circ$  in CY16–17.

As discussed in [5] and [11], the NaK population exhibits a predictable and stable cumulative RCS distribution due to the scattering characteristics of metallic spheres. The NaK population has been used successfully by the NASA ODPO as a secondary check on the calibration accuracy of the HUSIR debris data collects. For the Goldstone radar wavelength, it is expected that the NaK population will have a sudden increase in the cumulative count rate for particles with an RCS near  $-33.6$  dBsm. This increased count rate is due to the distribution of the radar cross section of the NaK particles in the Mie resonance region. The RCS for the case of Mie scattering for a sphere as a function of diameter at the Goldstone wavelength is shown in Fig. 6. In actual practice, this sharp bend in the cumulative RCS curve will be somewhat blurred, due to the inability to correct for the gain due to the distance of the debris path from the center of the beam.

By examining the cumulative RCS distributions of the NaK population and determining the deviation of the identifying feature from its expected location, an RCS calibration factor for each Goldstone dataset – CY16, CY17A, and CY17B – was calculated and applied uniformly across the dataset. Figure 7 shows the post-calibration SEM size estimate distributions for NaK identified by HUSIR and Goldstone in CY16-17. Goldstone’s CY16 and CY17 B are in good agreement with the HUSIR CY16-17 data. Due to remaining calibration issues, data from Goldstone CY17A will not be presented in subsequent plots. It should be noted that the SEM is used to compare results of radars that operate at different wavelengths and does not accurately reflect the size of a NaK droplet.

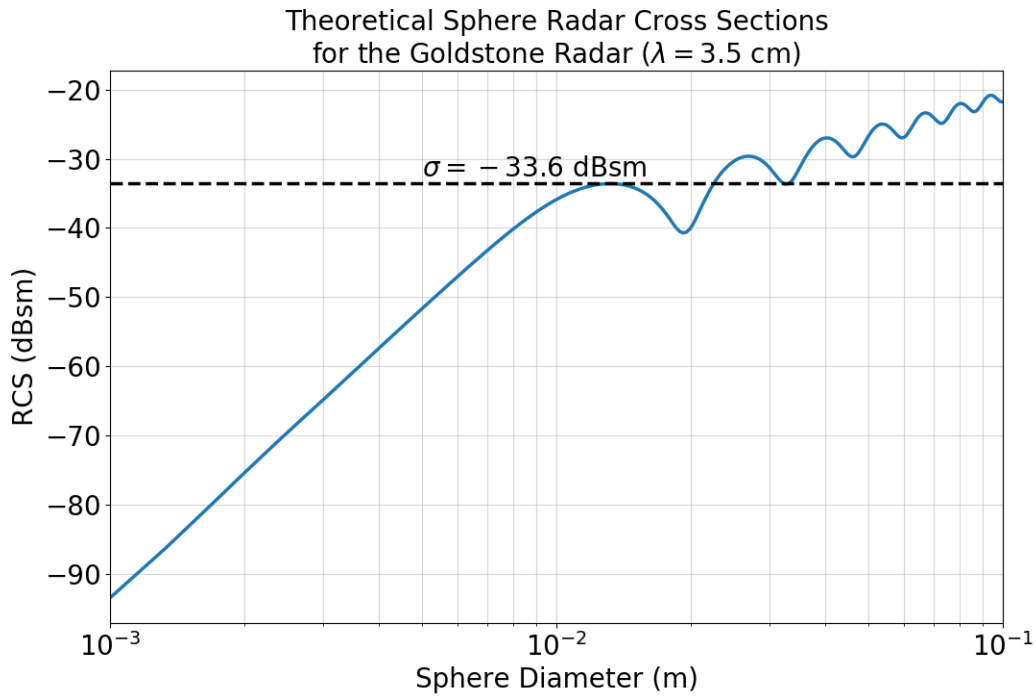


Fig. 6. Mie scattering for spheres at the Goldstone X-band wavelength. A reference line at -33.6 dBsm is shown, which is the RCS where a sudden change in the cumulative count rate for NaK is expected at the Goldstone wavelength.

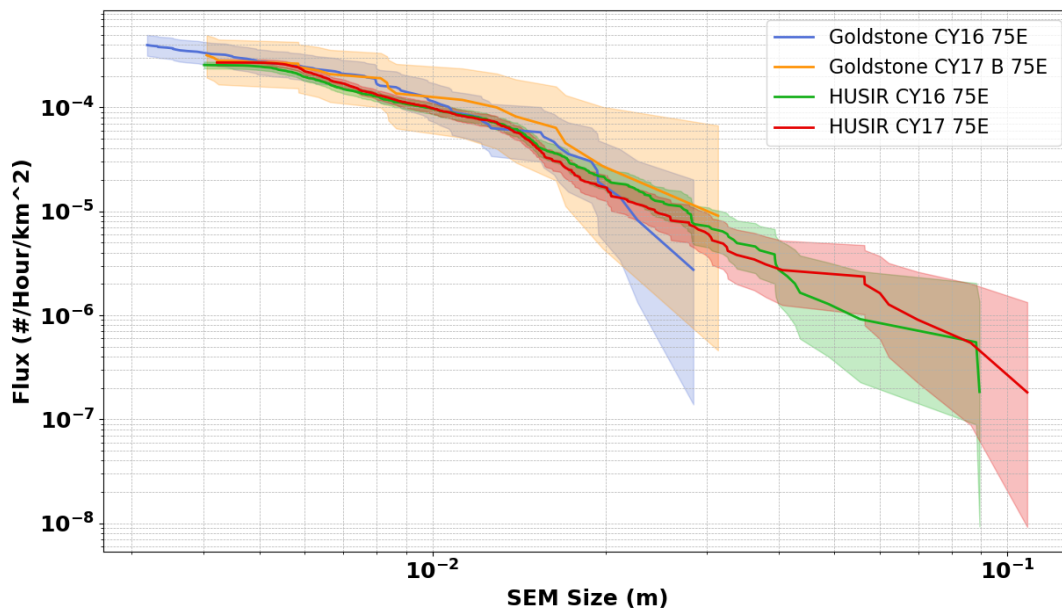


Fig. 7. Surface area flux of NaK particles versus SEM size estimate. SEM size is used to compare measurements made by radars operating at different wavelengths and does not accurately represent the physical diameter of spherical NaK droplets. The shaded regions represent the 95% confidence interval.

## 5 COMPARISON OF GOLDSTONE DATA TO HUSIR

Goldstone is useful to the NASA ODPO because it complements HUSIR by extending the measured cumulative flux curves to smaller sizes, about 3 mm in LEO as compared to 5 mm for HUSIR. Figure 8 shows the cumulative flux measured by HUSIR and Goldstone from 400 km to 1000 km in altitude in CY16-17. The two sensors are in good agreement between 5 mm and 1 cm. Below 5 mm the size distributions measured by HUSIR begin to roll off due to sensitivity limitations, whereas the Goldstone distributions do not begin to roll off until around 3 mm.

For sizes greater than 1 cm, the Goldstone CY16 distribution drops off. This is related to Goldstone's lack of Automatic Gain Control (AGC) on its receiver. This lack of AGC leads to saturation of the receiver for large returns, typically from larger objects, which horizontally compresses the cumulative size distributions. This effect is diminished in CY17 B, during which time Goldstone was operating at significantly reduced transmission power. Although it appears that the CY17 B flux distribution is not significantly affected by receiver saturation, the data still does not extend to sizes greater than 8 cm. Because Goldstone is unable to measure the location of the debris object within the beam, objects whose returns persist for longer than 90 milliseconds are removed as potential side lobe detections. This, coupled with reduced observation time, limits the measured Goldstone practical size distributions to smaller than 1 cm.

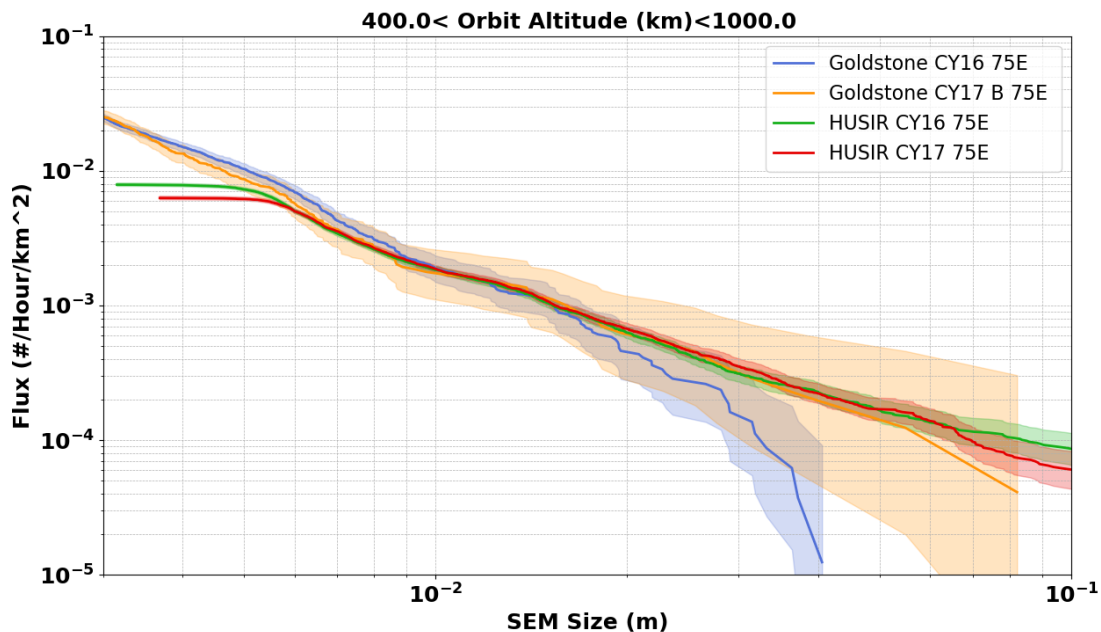


Fig. 8. Surface area flux of debris between 400 km to 1000 km altitude for the HUSIR and Goldstone radars. The shaded regions represent the 95% confidence interval.

## 6 SUMMARY

This paper presents measurements of the LEO orbital debris environment performed using Goldstone from CY16–17. In 2016, 3427 debris objects were detected over 46.3 hours of observations. In 2017, 3064 debris objects were detected over 51.8 hours of observations. The lower detection rate in 2017 is related to reduced transmission power during that year.

Several system upgrades implemented to improve the quality of measurements of the orbital debris environment were described. These improvements included changes to the bi-static observation geometry, receiver and transmitter bandwidth upgrades, and most recently at the end of 2015, the addition of a second receiver to enable recording of both polarizations (LCP and RCP) of the radar returns. This enabled, for the first time with Goldstone data, the discrimination of the NaK population based on polarization properties.



Goldstone is unable to measure the position of the detected object in the beam; therefore, the measured RCS is a lower bound of the true RCS and manifests as a bias in the measured RCS distributions. The unique scattering properties of the NaK population were used to develop a calibration factor to correct for this bias. The calibration was validated by comparison of the NaK population as measured by Goldstone to that measured by HUSIR. Using the calibrated Goldstone data, the cumulative size distributions for Goldstone and HUSIR for CY16–17 were compared for altitudes from 400 km to 1000 km and were shown to be in good agreement.

The new developments in data collection and analysis enable Goldstone to provide high fidelity orbital debris measurements and are invaluable in the characterization of the sub-centimeter debris population in LEO.

## 7 POST SCRIPT

On 28 February 2018, DSS-15, which has been used as the receiving antenna for Goldstone, was decommissioned. DSS-25 and DSS-26, two 34-m “Apollo” antennas, were identified as potential receiving antenna replacements for DSS-15. The baseline between DSS-14 and DSS-15 is approximately 497 m, which allowed that configuration to sample the entirety of LEO with a single pointing. The baseline between DSS-14 and DSS-25/DSS-26 is approximately 9.4 km, which restricts the altitude range over which the transmitter and receiver beams intersect. This makes the CY16-17 data presented the only dual polarization dataset from Goldstone that covers the entirety of LEO in a single pointing. Additional information regarding the new observation geometries employed using DSS-25 and DSS-26 as the receiving antenna can be found in [12].

## 8 REFERENCES

1. Anz-Meador, P., *et al.* “Sampling and Analysis of Impact Crater Residues found on the Wide Field Planetary Camera-2 Radiator,” Proc. 6th European Conf. Space Debris, 2013.
2. Squire, M.D., *et al.* “Joint Polar Satellite System (JPSS) Micrometeoroid and Orbital Debris (MMOD) Assessment,” NASA/TM-2015-218780, 2015.
3. Matney, M., *et al.* “Recent results from Goldstone orbital debris radar,” *Advances in Space Research* 23.1, pp. 5-12, 1999.
4. Goldstein, R.M. Summary of Goldstone Orbital Debris Observations: October 1996 to May 1997. *Telecommunications and Mission Operations Progress Report*, 133, pp.1-7, 1998.
5. Murray, J., *et al.* “Haystack Ultra-Wideband Satellite Imaging Radar Measurements of the Orbital Debris Environment: 2014-2017,” NASA/TP-2019-220302, 2019.
6. Goldstein, R. M., Goldstein, S. J., and Kessler, D. J. “Radar observations of space debris,” *Planetary and Space Science* 46.8, pp. 1007- 1013, 1998.
7. Lambour, R., *et al.* Assessment of Orbital Debris Size Estimation from Radar Cross-Section Measurements, *Adv. Space Res.*, v. 34, pp. 1013-1020, 2004.
8. Kessler, D. J. *et al.* “A Search for a Previously Unknown Source of Orbital Debris; the Possibility of Coolant Leak in RORSATs,” Proceedings of IAF, October 1997.
9. Grinberg, E. I., *et al.* “Interaction of Space Debris with Liquid Metal Circuit of RORSAT Satellites,” Proc. ESA, May 1997.
10. Lambour, R. and Sridharan, R. “Characteristic of an Anomalous Orbital Debris Population Inferred from Theoretical Modeling,” *J. of Spacecraft and Rockets*, v. 36, No. 5, Sept.-Oct. 1999.
11. Matney, M., *et al.* “The NaK Population: A 2019 Status,” International Orbital Debris Conference 2019, in work.
12. Murray, J. “New Geometry for Debris Observations using the Goldstone Orbital Debris Radar,” *Orbital Debris Quarterly News* Vol. 23, Issues 1 & 2, pp. 8, 2019.